

## Supporting Information

### Experimental section

#### Materials

Kevlar 49 yarns were purchased from Dupont and used after dried at 50 °C in vacuum for 12 h. Dimethyl sulfoxide (DMSO), potassium hydroxide (KOH), polyvinyl alcohol (PVA), aniline monomer, and ammonium persulphate (APS), 12M (mol/L) HCl were purchased from Sinopharm Chemical Reagent Co. Ltd. All reagents were of analytical grade and used as received without further purification.

#### Preparation of ANFs-PVA Hydrogels

Aramid nanofibers (ANFs)/DMSO dispersion were prepared according to the method reported in the reference.<sup>1</sup> Typically, bulk Kevlar 49 yarns (6.0 g) and KOH (9.0 g) were added to DMSO (300 mL) and stirred vigorously at room temperature for 3 weeks to obtain 20 mg/mL ANFs/DMSO dispersion. Then, 5 mL of ANFs/DMSO dispersion was mixed with an equal volume of a 100 mg/mL PVA ( $M_w$  145000–165000 a.u.) solution in DMSO. The mixture system was cast into a mold and immersed in water to form ANFs/PVA hydrogels with the desired shape.

#### Preparation of APP Hydrogels

The ANFs-PVA hydrogel with a size of  $1 \times 3 \times 0.03 \text{ cm}^3$  was immersed in 5 mL of 1 M HCl aqueous solution containing different initial concentrations of aniline monomer, and kept at 0 °C for 12 h. APS (mole ratio to aniline = 1:1, dissolved in 5 mL of 1 M HCl), pre-cooled to 0 °C, was poured into the above mixture, and the mixture was polymerized in situ at 0 °C. Finally, the composite hydrogel was thoroughly washed by HCl aqueous solution, ethanol and deionized water, respectively. According to the loading amount of polyaniline of 9.2 wt%, 14.7 wt%, 18.1 wt%, and 20.6 wt% (relative weight ratio of PANI to ANFs-PVA-PANI (APP) hydrogels), APP hydrogels (85% water content) were labeled as APP-0, APP-1, APP-2, APP-3 and APP-4, respectively.

#### Assembling of Strain Sensors Utilizing APP Hydrogels

To obtain the strain sensor, the excess water on the surface of APP-3 hydrogel ( $1 \times 3 \times$

0.05 cm<sup>3</sup>) was absorbed with filter paper, then two copper plates attached with conductive silver paste were connected to the both ends of the hydrogel (Figure 1).

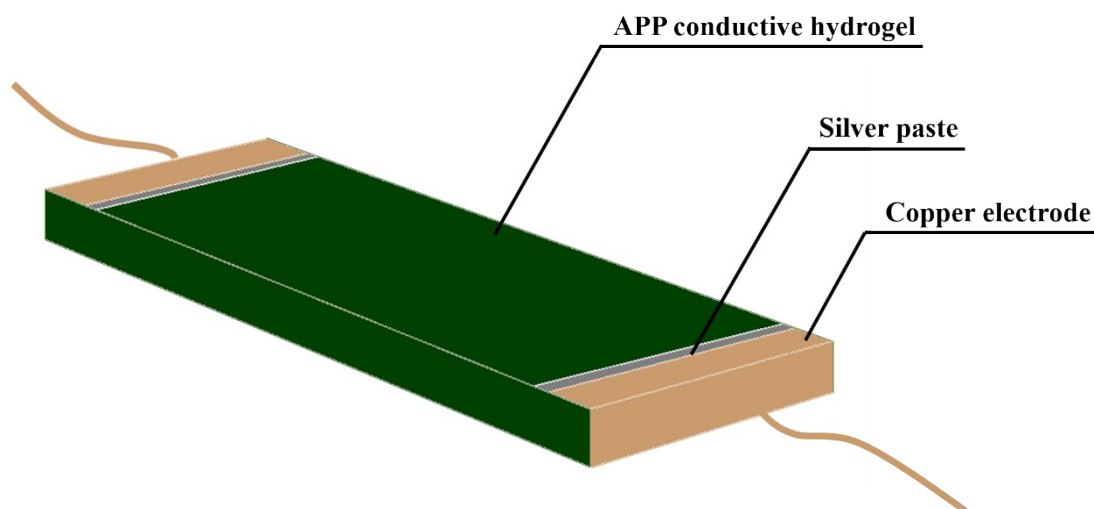


Fig. S1 Three-dimensional structure of strain sensors assembled from APP hydrogels.

### **Characterizations**

The fracture surface morphology of freeze-dried hydrogels was observed with field emission scanning electron microscopy (FE-SEM) (FEI-QUANTA250FEG, USA). Fourier transform infrared (FTIR) spectra were recorded on a Nicolet 8700 spectrometer (Thermo Fisher Scientific, USA) at a scanning resolution of 2 cm<sup>-1</sup> in the wavenumber range from 4000 to 500 cm<sup>-1</sup>. Raman spectrometer (Via-H31894, Renishaw, British) were performed in the wavenumber range from 400 to 2000 cm<sup>-1</sup>. X-ray diffraction (XRD) patterns were recorded on a D8-Advanced X-ray diffractometer (Bruker Co. Ltd, Switzerland) with Cu K $\alpha$  radiation ( $\lambda = 0.154$  nm) from 5 to 45°, at a scanning speed of 5° min<sup>-1</sup>. The oscillatory frequency sweep measurements were performed at a strain amplitude of 5 % with shear frequency in the range of 0.1–100 rad/s at 25 °C to determine the storage and loss moduli of the hydrogels. The tensile process of hydrogels was characterized using a universal tensile testing machine (CMT 4254, Shenzhen SANS, China) with a tensile rate of 1 mm min<sup>-1</sup> at ambient temperature. The conductivity of the hydrogel was tested by a digital source meter (Keithley 2400, Tektronix, U.S.A.), and the piezoresistive performance was also tested by it combining with a universal tensile testing machine. The digital source meter was applied to evaluate performance of APP hydrogel sensors in practical applications.

For ANFs, the characteristic bands at  $3313\text{ cm}^{-1}$  are attributed to the N-H stretching vibrations.<sup>2</sup> The bands at  $1631$  and  $1537\text{ cm}^{-1}$  are ascribed to the C=O stretching vibration and the N-H deformation vibration of amide group, respectively.<sup>3</sup> The bands at  $1501$  and  $1309\text{ cm}^{-1}$  are assigned to the C=C stretching and Ph-N stretching of benzene ring, respectively.<sup>4</sup> The characteristic peaks of PVA are presented for the ANFs/PVA hydrogels. The peaks at  $3286$ ,  $2904$ , and  $1083\text{ cm}^{-1}$  are attributed to the vibrations of O-H, C-H, and C-O bonds of PVA, respectively.<sup>5,6</sup> In ANFs-PVA composite materials, the C=O characteristic peak of ANFs obviously moves to the low band, which proves the existence of hydrogen bond between ANFs and PVA components.<sup>2</sup>

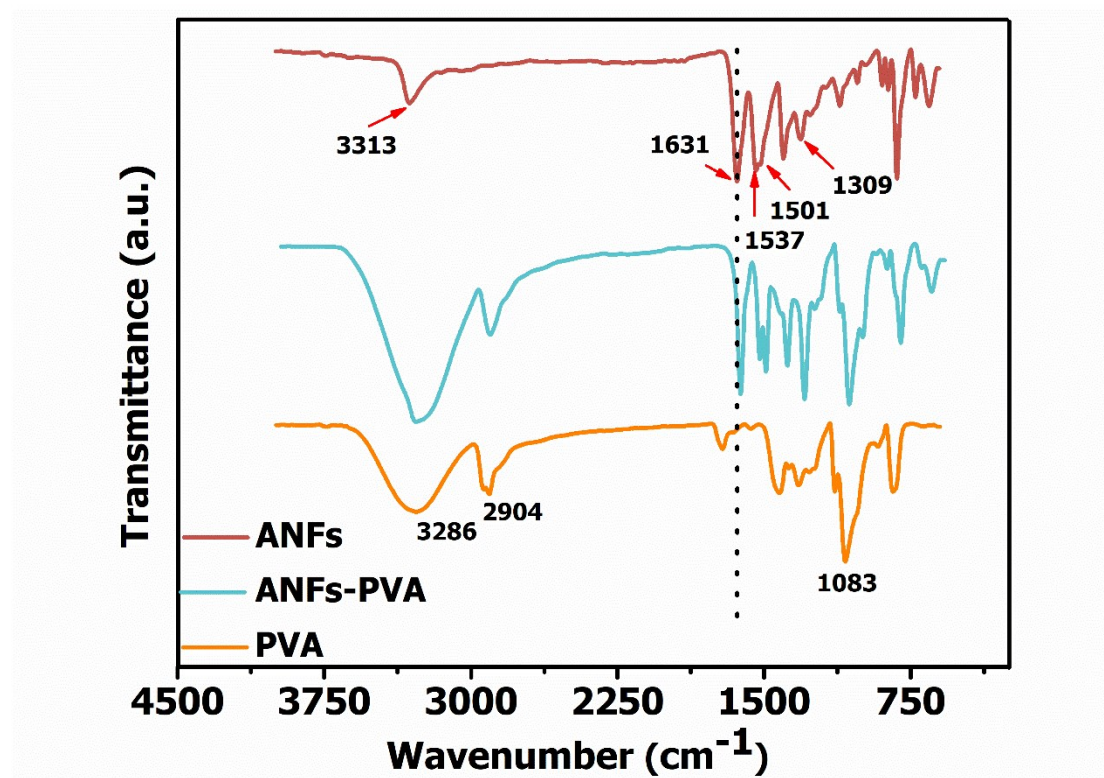


Fig. S2 FTIR spectra of ANFs, PVA and ANFs-PVA

X-ray diffraction spectroscopy (XRD) scans of PVA, ANFs, PANI and APP hydrogels are shown in Figure S3 (Supporting Information). In the X-ray diffraction curve of PVA, the crystalline peaks appear at  $2\theta = 19.5^\circ$ , corresponding to the (101) plane of the PVA.<sup>6</sup> The ANFs shows three typical Kevlar characteristic peaks, which

can be assigned to the (110), (200), and (004) diffractions, respectively.<sup>2</sup> For the PANI, two broad peaks at around  $2\theta = 20.6$  and  $25.1^\circ$  are ascribed to the periodicity parallel and perpendicular to PANI chains.<sup>3</sup> In the case of APP, the main characteristic peak was consistent with ANFs, but the intensity decreased significantly, which may be attributed to the introduction of the PVA and PANI.<sup>4</sup>

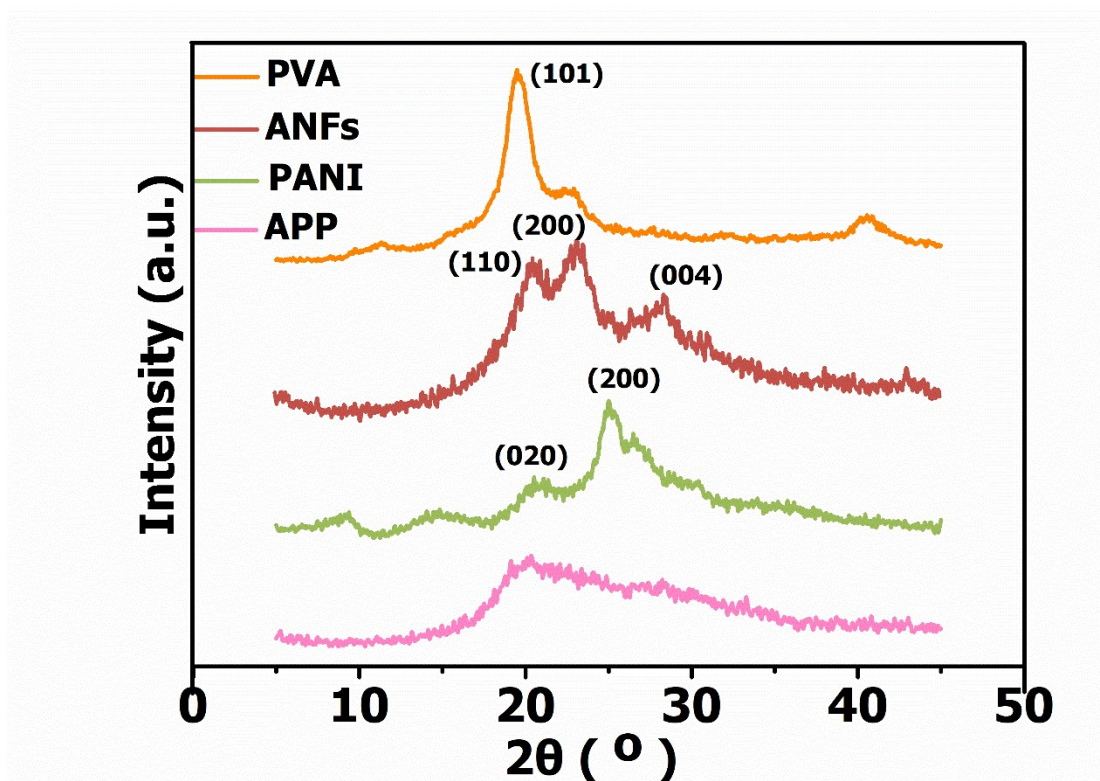


Fig. S3 XRD spectra of PVA, ANFs, PANI and APP.

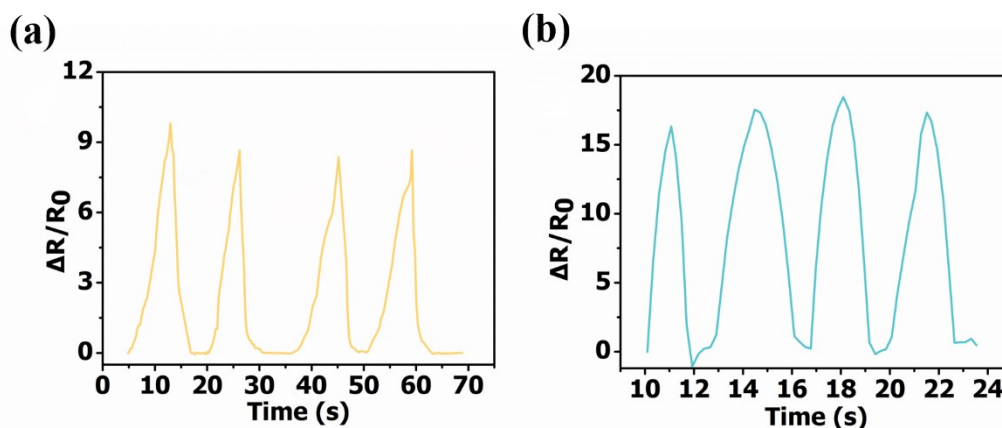


Fig. S4 (a) The stretching cycle at 60% strain. (b) The stretching cycle at 100% strain.

## References

1. Yang, M.; Cao, K.; Sui, L.; Qi, Y.; Zhu, J.; Waas, A.; Arruda, E. M.; Kieffer, J.; Thouless, M. D.; Kotov, N. A., Dispersions of Aramid Nanofibers: A New Nanoscale Building Block. *Acs Nano* 2011, 5 (9), 6945–6954.
2. Yang, B.; Wang, L.; Zhang, M.; Luo, J.; Ding, X., Timesaving, High-Efficiency Approaches To Fabricate Aramid Nanofibers. *ACS Nano* 2019, 13 (7), 7886-7897.
3. Cao, K.; Siepermann, C. P.; Yang, M.; Waas, A. M.; Kotov, N. A.; Thouless, M. D.; Arruda, E. M., Reactive Aramid Nanostructures as High-Performance Polymeric Building Blocks for Advanced Composites. *Advanced Functional Materials* 2013, 23 (16), 2072-2080.
4. Yin, Q.; Jia, H.; Mohamed, A.; Ji, Q.; Hong, L., Highly Flexible and Mechanically Strong Polyaniline Nanostructure @ Aramid Nanofiber Films for Free-standing Supercapacitor Electrodes. *Nanoscale* 2020.
5. Li, W.; Lu, H.; Zhang, N.; Ma, M., Enhancing the Properties of Conductive Polymer Hydrogels by Freeze–Thaw Cycles for High-Performance Flexible Supercapacitors. *ACS Applied Materials & Interfaces* 2017, 9 (23), 20142-20149.
6. Li, W.; Lu, H.; Zhang, N.; Ma, M., Enhancing the Properties of Conductive Polymer Hydrogels by Freeze–Thaw Cycles for High-Performance Flexible Supercapacitors. *ACS Applied Materials & Interfaces* 2017, 9 (23), 20142-20149.
7. Xu, L.; Zhao, X.; Xu, C.; Kotov, N. A., Water-Rich Biomimetic Composites with Abiotic Self-Organizing Nanofiber Network. *Adv Mater* 2018, 30 (1).
8. Hu, C.; Zhang, Y.; Wang, X.; Xing, L.; Shi, L.; Ran, R., Stable, Strain-Sensitive Conductive Hydrogel with Antifreezing Capability, Remoldability, and Reusability. *ACS Appl Mater Interfaces* 2018, 10 (50), 44000-44010.